Contribution from the Department of Materials Science and Engineering and the Department of Chemistry, Massachusetts Institute of Technology, Cambridge, Massachusetts 02139

Reductive Elimination of HH, HCH_3, and CH_3CH_3 from Bis(phosphine)platinum(II), -palladium(II), and -nickel(II) Complexes: A Theoretical Study Using the SCF-Xα-SW Method

ANNA C. BALAZS, KEITH H. JOHNSON, and GEORGE M. WHITESIDES*

Received March 5, 1981

Self-consistent-field-Xα-scattered-wave (SCF-Xα-SW) calculations have been carried out for the two series of organometallic complexes (L = H_3P) L_2PtH_2, $L_2Pt(H)CH_3$, and $L_2Pt(CH_3)_2$ and $L_2Ni(CH_3)_2$, $L_2Pd(CH_3)_2$, and $L_2Pt(CH_3)_2$. These calculations suggest a correlation between the relative rates of reductive elimination ($L_2MXY \rightarrow L_2M + XY$) and the molecular orbital character of the starting complexes: those compounds which eliminate XY relatively rapidly have occupied molecular orbitals with pronounced M-X(Y) antibonding character; those which eliminate XY slowly have only vacant M-X(Y) antibonding orbitals. No single orbital (HOMO or other) dominates the M-X(Y) bonding in these complexes: bonding and antibonding character is distributed among several of the valence orbitals. We propose a simple model to correlate the occupancy of antibonding M-X(Y) orbitals and rates of reductive elimination with the relative electronegativities of M and X(Y). The limitations of this model, and alternates to it, are described briefly.

Introduction

This paper outlines a theoretical study of the electronic structure of several transition-metal organometallic compounds having the structure $(H_3P)_2MXY$ (X, Y = H, CH_3) carried out with the self-consistent-field-Xα-scattered-wave (SCF-Xα-SW) method. It examines the characteristics of the upper occupied molecular orbitals of these complexes and looks for correlations between these characteristics and the relative rates of reductive elimination of the elements of XY from them (eq 1, L = PH_3). These reactions, and the reactions which are

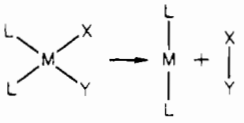

(1)

M = Pt, Pd, Ni
X, Y = H, CH_3

their microscopic reverse are models for the individual steps in a number of useful processes catalyzed by transition metals (homogeneous hydrogenation, coupling, and reduction; perhaps heterogeneous hydrogenation and dehydrogenation).[1]

The calculations described here were stimulated by two qualitative generalizations which are emerging from current experimental work in the organometallic chemistry of the d^8 metals. First, the rates of the reductive elimination reactions of the type represented by eq 1 appear to decrease in the order $k_{L_2MH_2} > k_{L_2M(H)CH_3} > k_{L_2M(CH_3)_2}$ for a series in which the metal and its ligands L are constant. Second, the rates of these reactions seem to increase in the order $k_{L_2Pt(CH_3)_2} < k_{L_2Pd(CH_3)_2} < k_{L_2Ni(CH_3)_2}$ in a series in which only the metal changes.[2-4] Unfortunately, there are presently few strictly comparable examples in either series, and the value of these generalizations remains to be established. Further, we must assume that those reductive eliminations which are known follow the same mechanism and are concerted in order to compare their rates.[5] These assumptions are probably correct for many cases, but convincing experimental evidence supporting their correctness exists in only a few cases.[2-4,6] Their uncertain generality notwithstanding, these two series serve as a starting point for theoretical consideration of this type of chemistry.

At the outset, we acknowledge that this work is directed to only one of several factors which might in principle influence the relative rates in these series: viz., the electronic structure of the L_2MXY group. Entropic effects (which are probably similar for all the reactions subsumed by eq 1[7]) and nonbonded steric effects (which may be significantly different for different of these reactions[8]) are neglected entirely. We touch only briefly on differences in the energies of the assumed products (L_2M, X-Y) and make no estimates of energies of transition states. Limitations intrinsic to the version of the SCF-Xα-SW method used here further constrain the types of questions concerning local electronic structure which can be addressed (see below). The objective of the work is thus *not* to discuss which features of the electronic structure of the metal and its directly bonded ligands *determine* the relative rates of eq 1, or even to try to establish whether this electronic structure does in fact dominate these rates. Addressing either question would require the ability to construct potential surfaces (including enthalpic contributions due to nonbonded interactions and entropic terms) describing the decompositions in a detail which is presently beyond the capability of this (and other) theoretical methods. Instead, the objective of this work is to explore the limited question of whether the trends in rates *correlate* with physically interpretable characteristics of the local electronic

(1) Gates, B. C.; Katzer, J. R.; Schmit, G. C. A. "Chemistry of Catalytic Processes"; McGraw-Hill: New York, 1979. Webster, D. E. *Adv. Organomet. Chem.* **1977**, *15*, 147-188. Sinfelt, J. H. *Science (Washington, D.C.)* **1977**, *195*, 641-646. Clarke, J. K. A.; Rooney, J. J. *Adv. Catal.* **1976**, *25*, 125-183. Parshall, G. W. "Homogeneous Catalysis"; Wiley-Interscience, New York, 1980.

(2) Pt: McCarthey, T. J.; Nuzzo, R. G.; Whitesides, G. M. *J. Am. Chem. Soc.* **1981**, *103*, 1676-1678. Young, G. B.; Whitesides, G. M. *Ibid.* **1978**, *100*, 5808-5815. Foley, P.; DiCosimo, R.; Whitesides, G. M. *Ibid.* **1980**, *102*, 6713-6725. Abis, L.; Sen, A.; Halpern, J. *Ibid.* **1978**, *100*, 2915-2916. Braterman, P. S.; Cross, R. J.; Young, G. B. *J. Chem. Soc., Dalton Trans.* **1976**, 1306-1310, 1310-1314.

(3) Pd: Ozawa, F.; Ito, T.; Yamamoto, submitted for publication in *J. Am. Chem. Soc.* Milstein, D.; Stille, J. K. *Ibid.* **1979**, *101*, 4981-4991. Gillie, A.; Stille, J. K., submitted for publication in *J. Am. Chem. Soc.*

(4) Ni: Grubbs, R. H.; Miyashita, A. *J. Amer. Chem. Soc.* **1978**, *100*, 7416-7418, 7418-7420. Yamamoto, T.; Yamamoto, A., Ikeda, S. *Ibid.* **1971**, *93*, 3350-3359; 3360-3364.

(5) Other possible processes which might result in reductive elimination include free radical pathways (Whitesides, G. M.; Bergbrecter, D.; Kendall, P. E. *J. Am. Chem. Soc.* **1976**, *96*, 2806-2813. Kochi, J. K. In "Free Radicals"; Wiley-Interscience: New York, 1973; Vol. 1, Chapter 11), bimolecular processes or cluster processes (Norton, J. R. *Acc. Chem. Res.* **1979**, *12*, 139-145 and references cited therein); electron-transfer reactions (Tsou, T. T.; Kochi, J. K. *J. Am. Chem. Soc.* **1978**, *100*, 1634-1635), paths requiring prior oxidative addition (Brown, M. P.; Puddephatt, R. J.; Upton, C. E. E. *J. Chem. Soc., Dalton Trans.* **1974**, 2456-2465), and reactions involving compositions and geometries different from the ground state (Grubbs, R. H.; Miyashita, A.; Liu, M.; Burk, P. *J. Am. Chem. Soc.* **1978**, *100*, 2418-2425. Glockling, F.; McBride, T.; Pollock, R. J. *T. J. Chem. Soc., Chem. Commun.* **1973**, 650 and ref 2-4).

(6) Komiya, S.; Albright, T. A.; Hoffmann, R.; Kochi, J. K. *J. Am. Chem. Soc.* **1976**, *98*, 7255-7265.

(7) Benson, S. W. "Thermochemical Kinetics"; Wiley: New York, 1968; Chapter 3.

(8) Tolman, C. A. *Chem. Rev.* **1977**, *77*, 313-348.

0020-1669/82/1321-2162$01.25/0

structure of the reactants, L_2MXY. If such correlations exist and can be identified, they may be useful in guiding the synthesis of mechanistically or synthetically useful organometallic complexes. Any more sophisticated effort to distinguish between "correlation" and "cause" in this area of organometallic chemistry must be postponed until more and better experimental data (especially data establishing the structures of typical transition states) and more accurate theoretical methods are available.

Previous theoretical discussions of rates of reductive elimination reactions include works by Hoffmann et al.,[9] Braterman and Cross,[10] and Åkermark.[11] Additional relevant calculations have been described by Goddard, Anderson, and others.[12]

Methods

Calculations were carried out with the SCF–Xα–SW method described elsewhere.[13] The general strengths and weaknesses of this method have been summarized by Salahub et al.[14] Here we emphasize only points which are relevant to the particular problem being explored. The SCF–Xα–SW method has two strengths vis à vis other theoretical methods. First, it can calculate wavefunctions and *relative* energies of orbitals for many-electron systems economically and provides good wavefunctions for species characterized by pronounced ionic character in bonds. It is thus practical to use this method to examine organometallic compounds containing heavy elements such as platinum, palladium, and nickel. The ability to calculate electron distributions in orbitals is especially useful in identifying those orbitals which contribute significantly to the bonding (or antibonding) of the metal to its ligands. This type of identification is not always obvious, especially when, as in the complexes examined here, bonding is distributed among several orbitals rather than localized in one. Second, the eigenvalues generated in a calculation can be related directly to orbital electronegativity and provide a characterization of the electronic structure which is obtained with more difficulty using other methods. The *relative* energies of orbitals (that is, the differences in energy between them) are calculated relatively well with the SCF–Xα–SW method, and one of the most useful applications of the method has been in the calculation of electronic absorption spectra for transition-metal complexes (with use of the "transition state" method).[13,15]

The present SCF–Xα–SW calculations have the important weakness that they give unreliable *total* electronic energies of molecules. They are thus unsuitable for the calculation of potential surfaces and for problems which require energy minimization. The type of calculation employed in this paper is not, for example, capable of estimating ground-state geometries[16] and certainly cannot be used to estimate structures or energies of transition states. It cannot, therefore, calculate the quantity of most direct interest in any study of reaction rates—that is, the difference in energy between ground and transition states (the activation energy). Efforts to use the SCF–Xα–SW method at this level to examine problems in kinetics must thus rely on inferences based on the (known or estimated) ground-state structures of the reactants and products and on the energy, symmetries, and shapes of the orbitals of these materials. Orbital correlation diagrams have been employed as an aid in similar analyses employing other types of molecular orbital calculations. As we shall show, and in agreement with previous work,[9] they are relatively unin-

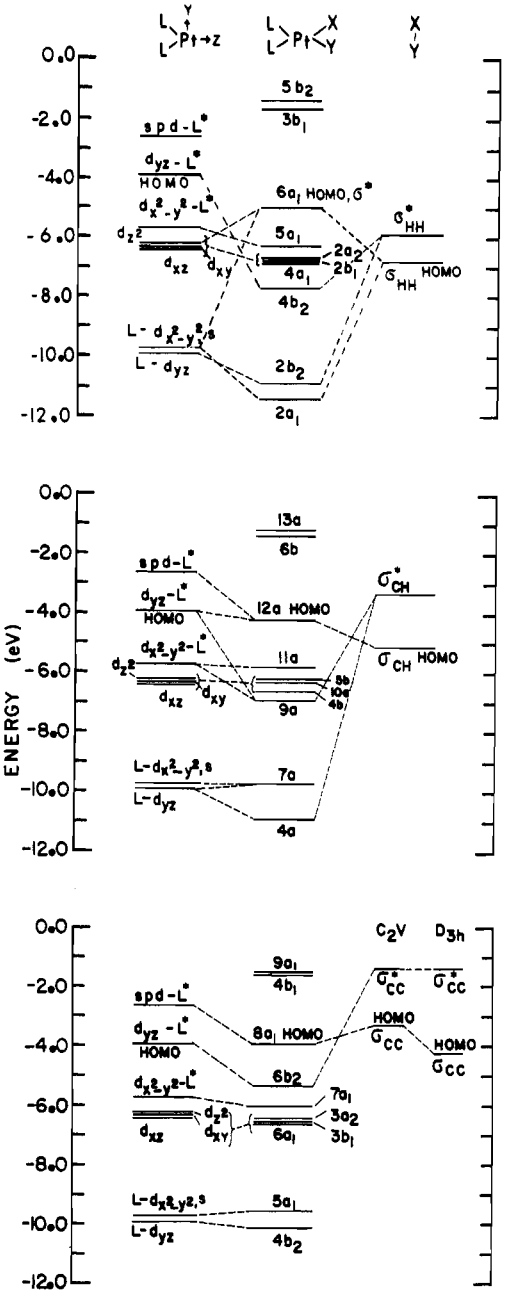

Figure 1. Eigenvalues for L_2PtXY [XY = HH (top), CH_3H (middle), CH_3CH_3 (bottom)]. Only the orbitals of L_2Pt and XY making major contributions to the molecular orbitals of L_2PtXY are indicated. The eigenvalues for XY are those calculated at the distances assumed in the complex (r_{HH} = 2.80 Å, r_{CH_3-H} = 2.73 Å, $r_{CH_3-CH_3}$ = 2.72 Å). In addition, the eigenvalues for CH_3CH_3 are also calculated from the bent geometry (C_{2v} symmetry) this moiety displays in the $L_2Pt(CH_3)_2$ complex. Calculations of the distorted CH_3–H molecule displaying both C_{3v} and C_s symmetries revealed insignificant differences. The figure displays the eigenvalues obtained from the CH_3–H fragment having C_{3v} symmetry. L = PH_3 in each case.

(9) Tatsumi, K.; Hoffmann, R.; Yamamoto, A.; Stille, J. K. *Bull. Chem. Soc. Jpn.*, in press. Hoffmann, R., submitted for publication in *Science* (*Washington, D.C.*). Gillie, A.; Stille, J. K. *J. Am. Chem. Soc.* **1980**, *102*, 4933–4937.

(10) Braterman, P. S.; Cross, R. J. *Chem. Soc. Rev.* **1973**, *2*, 271–294.

(11) Åkermark, B.; Ljungquist, A. *J. Organomet. Chem.* **1979**, *182*, 59–75. Åkermark, B.; Johansen, H.; Roos, B.; Wahlgren, U. *J. Am. Chem. Soc.* **1979**, *101*, 5876–5883.

(12) Anderson, A. B. *J. Am. Chem. Soc.* **1978**, *100*, 1153–1159. Upton, T. H.; Goddard, W. A., III. *Ibid.* **1978**, *100*, 321–323. Rappé, A. K.; Goddard, W. A., III. *Ibid.* **1977**, *99*, 3966–3968. Moll, J. O.; Hay, P. J., submitted for publication in *J. Am. Chem. Soc.*

(13) Slater, J. C.; Johnson, K. H. *Phys. Rev.* **1972**, *B5*, 844–853. Johnson, K. H. *Annu. Rev. Phys. Chem.* **1975**, *26*, 39–57. Slater, J. C. "The Self-Consistent Field for Molecules and Solids", Vol. 4 of "Quantum Theory of Molecules and Solids"; McGraw-Hill: New York, 1974; p 101 ff. Johnson, K. H. *Adv. Quantum Chem.* **1973**, *7*, 143–185.

(14) Salahub, D. R.; Foti, A. E.; Smith, V. H. *J. Am. Chem. Soc.* **1978**, *100*, 7847–7859.

(15) Noodleman, L. *J. Chem. Phys.* **1976**, *64*, 2343–2349.

(16) Danese, J. B.; Connally, J. W. D. *J. Chem. Phys.* **1974**, *61*, 3063–3070. Danese, J. B. *Ibid.* **1974**, *61*, 3071–3080. Cook, M. Ph.D. Thesis, Harvard University, 1981, unpublished.

formative in the particular problem chosen here.

In order to use oribtal correlation diagrams in any fashion, it is necessary to be able to calculate orbital energies with useful accuracy. The fact that the version of the SCF–Xα–SW program used here can estimate *individual* orbital energies usefully but that it cannot estimate *total* electronic energies deserves some explanation. So that rapid computation could be facilitated, an additional approximation is introduced in calculating the Xα total energy that is not made in calculating individual orbital energies: the charge density generated from the one-electron wavefunctions is spherically averaged within the atomic sphere boundaries and assumed to be a constant in the region between the spheres. This procedure introduces major errors in the value of the total energy. Dramatic improvements of the total energy have been achieved when the full, unaveraged, charge density generated is used in evaluating the Xα total energy.[16] These improvements suggest that the discrepancies between total energies calculated in the Xα–SW model and experiment are caused mainly by the approximation of a spherical charge distribution and are not a reflection of intrinsic defects in the Xα method.

The geometries chosen for the five complexes studied are these:

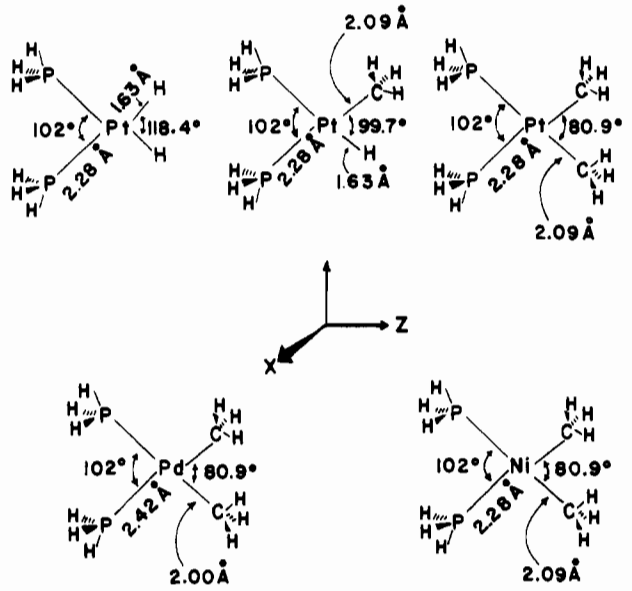

These distances and angles are unfortunately poorly based in detailed experimental precedent but are sufficiently accurate to examine qualitative trends in the complexes involved.[17] In any event, these choices resemble closely those used by Hoffmann et al.[9] in a useful study of reductive elimination and facilitate comparison between the results of these studies.

Calculations

Schwarz's α_{HF} values[18] were used for the atomic exchange parameters, except for hydrogen, for which 0.777 25 was used.[19] For the extramolecular and intersphere regions, a weighted average of the atomic α's was employed, the weights being the number of *valence* electrons in neutral atoms. Overlapping sphere radii were used.[20,21]

So that a check on the consistency of the parameters used for carbon and hydrogen could be provided, the transition state method was used to calculate the first ionization potentials for dihydrogen, methane, and ethane. These values (eV), together with experimental values,[22] are as follows: H_2, 17.6, 15.4; CH_4, 12.7, 12.6; C_2H_6, 11.0, 11.5. A similar calculation for the metals gives the following (calcd, obsd): Pt, 8.77, 9.00; Pd, 8.57, 8.33; Ni, 7.89, 7.63.[22,23] Using the same method, Parr et al. have calculated the electron affinities for the elements up to atomic number 54 with a similar level of agreement.[24] Comparison of these several experimental and calculated values suggest the values calculated by the SCF–Xα–SW method to be uncertain by about 1 eV. We place this level of agreement between calculated and experimental numbers in perspective by noting that it is unlikely that the *total* spread in values for $\Delta G^{\ddagger}$ for the reductive elimination of XY from the L_2MXY complexes studied here exceeds 1 eV. Thus, the uncertainty in *quantitative* precision of the computational method is approximately the same as the magnitude of the phenomenon being studied; accordingly, only *qualitative* trends in the calculations are interpretable.

Atomic charges were calculated with a qualitative procedure and are useful only for comparisons: the absolute values are not reliable.[25] The intersphere and extramolecular charge was partitioned among the atomic centers in proportion to the intrasphere charges. That is, atomic charges were estimated by normalizing the total number of valence electrons within all the atomic spheres to the total number for the molecule. The sphere sizes for a particular element also vary slightly from compound to compound; this variation also complicates quantitative interpretation of calculated charge distributions.

Results

L_2PtH_2, $L_2Pt(H)CH_3$, and $L_2Pt(CH_3)_2$. Figure 1 gives calculated eigenvalues. Only orbitals involved in bonds between P, Pt, and X(Y) (and nonbonding d orbitals on Pt) are shown; inner-shell orbitals and P–H and methyl C–H bonds

(17) The r_{PtP} and PPtP angle used were taken from $(Ph_3P)_2Pt(PhC{\equiv}CPH)$ (Glanville, J. O.; Steward, J. M.; Grim, S. O. *J. Organomet. Chem.* **1967**, *7*, P9–P10); r_{PH} and HPH angle were from PH_3 (Sirvetz, M. H.; Weston, R. E., Jr. *J. Chem. Phys.* **1953**, *21*, 898–902). These same dimensions were used in L_2PtH_2, $L_2Pt(CH_3)_2$, $L_2Pt(H)CH_3$, and $L_2Ni(CH_3)_2$. The value of r_{PtH} was taken to be the sum of platinum and hydrogen covalent radii (1.35, 0.25 Å) (Frenz, B. A.; Ibers, J. A. In "Transition Metal Hydrides"; Muetterties, E. L., Ed.; Marcel Dekker: New York, 1971; p 33). The r_{HH} was taken as the sum of the ionic radii (1.40 Å) (Libowitz, G. G. "The Solid-State Chemistry of Binary Metal Hydrides"; W. A. Benjamin: New York, 1965; p 7; Ladd, M. F. C. *Theor. Chim. Acta* **1968**, *12*, 333–336). This choice yields for the HPtH angle 118.4°. The r_{PtC} was the average r_{PtC} in $(Ph_3P)_2\overrightarrow{Pt(CH_2)_3CH_2}$ (Biefield, C. G.; Eecle, H. A.; Grubbs, R. H. *Inorg. Chem.* **12**, 2166–2170); the CPtC angle was also taken from this complex. The bond lengths in $L_2Ni(CH_3)_2$ were taken as the same as those of $L_2Pt(CH_3)_2$, in the absence of close analogy. Similar distances and angles are seen in related complexes (Jolly, P. W.; Wilke, G. "The Organic Chemistry of Nickel"; Academic Press: New York, 1974; Vol. 1, p 197. Cook, C. D.; Koo, C. H.; Nyburg, S. C.; Shiomi, M. T. *Chem. Commun.* **1967**, 426–427). The r_{PdC} and r_{PdP} bond lengths were from Mathis (Mathis, P. M. "The Organic Chemistry of Palladium"; Academic Press: New York, 1971; Vol. 1, p 39). Angles in $L_2Pd(CH_3)_2$ were the same as those in $L_2Ni(CH_3)_2$.

(18) Schwarz, K. *Phys. Rev. B.* **1972**, *5*, 2466–2468; *Theor. Chim. Acta* **1974**, *34*, 225–231.
(19) Slater, J. C. *Int. J. Quantum Chem.* **1973**, *7S*, 533–544.
(20) Norman, J. G., Jr. *J. Chem. Phys.* **1974**, *61*, 4630–4635; *Mol. Phys.* **1976**, *31*, 1191–1198.
(21) Atomic and outer-sphere radii (bohrs): for $Pt(PH_3)_2$, outer 7.620, Pt 2.522, P 2.208, H 1.440; for $(PH_3)_2PtH_2$, outer 7.878, Pt 2.522, H 1.440, P 2.208, and Hp 1.440; for $(PH_3)_2Pt(CH_3)H$, outer 7.620, Pt 2.530, H 1.460, C 1.770, H_C 1.250, P 2.330 and Hp 1.440; for $(PH_3)_2Pt(CH_3)_2$, outer 7.620, Pt 2.522, C 1.707, H_C 1.239, P 2.208, and Hp 1.440; for $(PH_3)_3Ni(CH_3)_2$, outer 7.620, Ni 2.440, C 1.770, H_C 1.250, P 2.300, and Hp 1.440; for $(PH_3)_3Pd(CH_3)_2$, outer 7.872, Pd 2.381, C 1.784, H_C 1.249, P 2.356, and Hp 1.443.
(22) Weast, R., Ed. "Handbook of Chemistry and Physics"; Chemical Rubber Co.; Cleveland, OH, 1969; pp E-80 (C, H), E-74 (Pt, Pd, Ni).
(23) For transition-state configurations the following were assumed: Pt ($d^{9.5}$), Pd ($d^{9.5}$), and Ni ($d^{8.5}s^{1.5}$). The configuration used for nickel was that recommended by Schwartz (Schwartz, K. *J. Phys. B* **1978**, *11*, 1339–1351).
(24) Bartolotti, L. J.; Gadre, S. R.; Parr, R. G. *J. Am. Chem. Soc.* **1980**, *102*, 2945–2948.
(25) Although the charge distributions estimated in this method are not highly accurate, they seem to be in general agreement with values estimated experimentally: Chatt, J.; Leigh, G. J. *Angew. Chem., Int. Ed. Engl.* **1978**, *17*, 400–407.

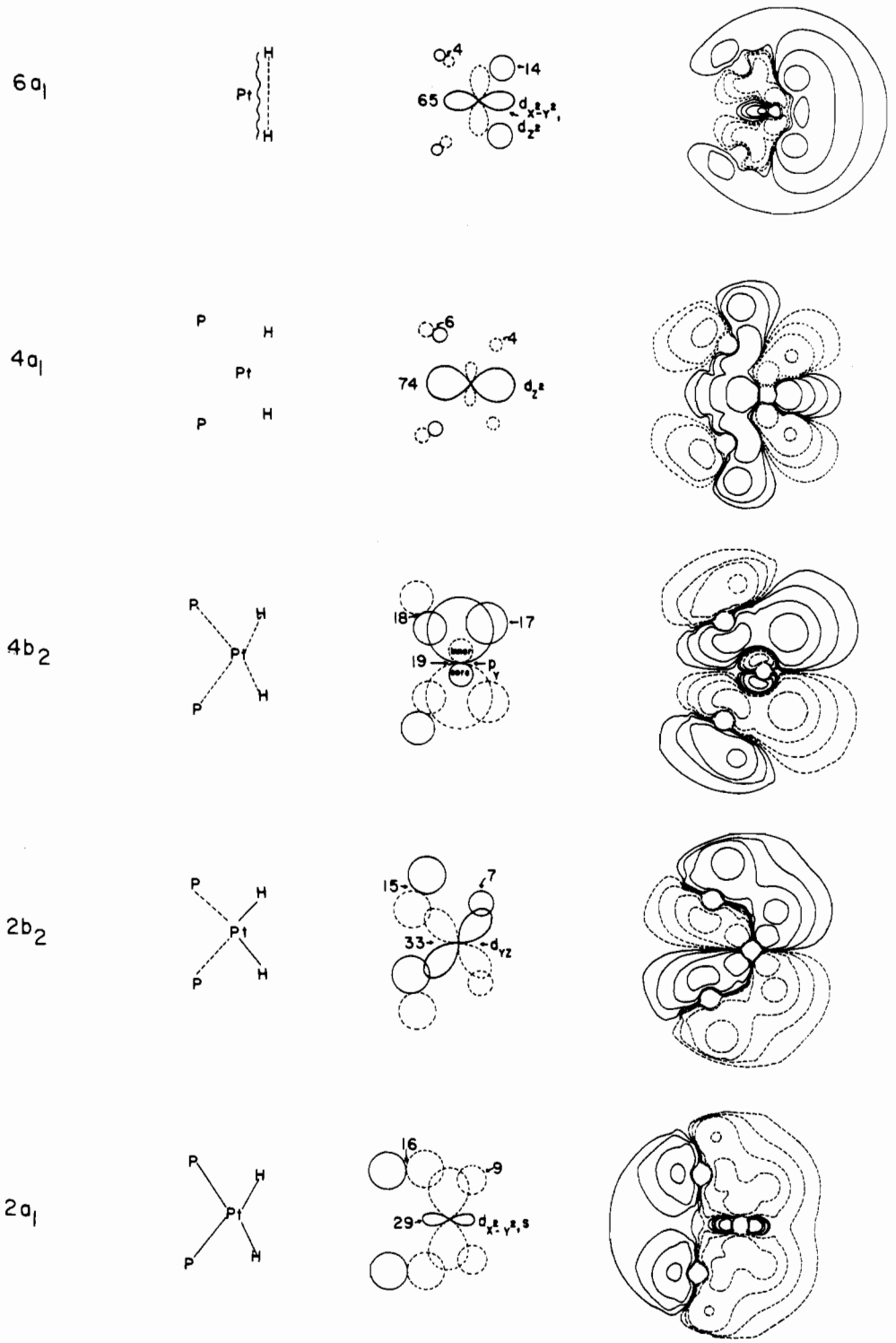

Figure 2. Orbitals important to bonding in L_2PtH_2. The first column represents the simplified interpretation of the bonding in the orbital: —, strongly bonding; ---, weakly bonding; ⁓, strongly antibonding. Thus, for example, the $2b_2$ orbital has strong Pt–H bonding character and weak Pt–P bonding. The two hydrogens (and the two phosphorus atoms) are weakly antibonding with respect to one another. No line between nearest-neighbor atoms (as between Pt and P in the $4a_1$ orbital) indicates a weak or nonbonding interaction. If a center is omitted from the diagram, the charge assigned to it is considered sufficiently small that it effectively does not participate in the orbital. The second column sketches the orbital makeup in terms of atomic orbitals. The numbers represent the fractional charge (expressed as a percentage of two electrons) centered on each center. These charges do not add to 100 because the charge on the hydrogens in PH_3 and CH_3 have been omitted from the diagram. The major contributions of the orbitals on platinum are indicated on the diagram. For example, the $2a_1$ orbital contains important contributions from d_{z^2} and s orbitals centered on platinum. The last column contains a section through the wave function. The contours are plotted at values of ±0.003, ±0.009, ±0.027, and ±0.081, starting from the outermost.

are omitted. Figures 2–4 summarize the composition of important molecular orbitals ("important" is defined by the orbital correlation diagrams as orbitals involved in bonds which are made or broken during elimination of XY from L_2PtXY; see below).

For comparison, Figure 5 gives similar information for L_2Pt^0. Reductive elimination of XY from L_2PtXY with generation of L_2Pt^0 is certainly accompanied by a spreading of the L–Pt–L angle. We cannot estimate the value of this angle at the transition state. Figure 5 arbitrarily gives orbitals

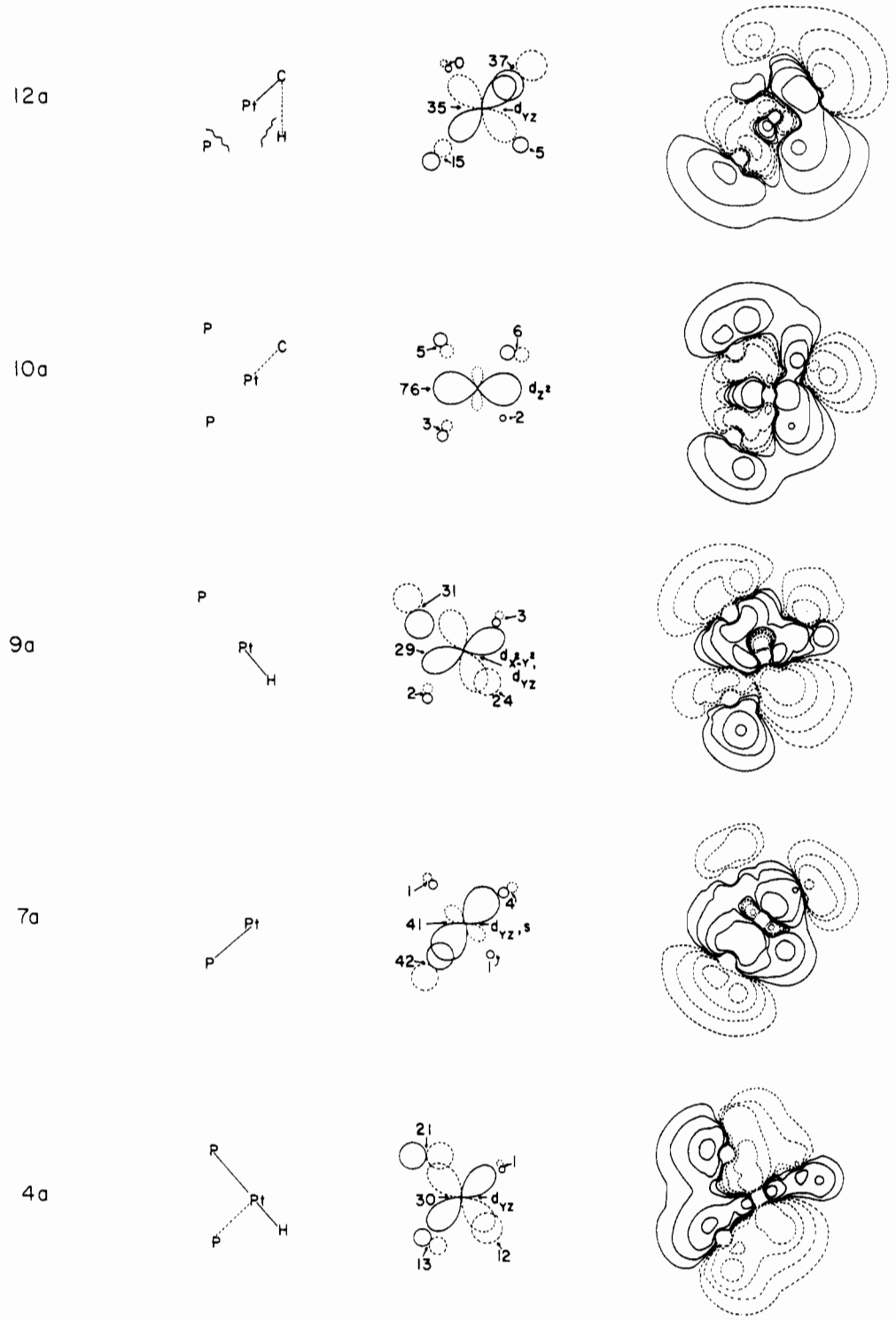

Figure 3. Orbitals important to bonding in $L_2Pt(H)CH_3$. The caption for Figure 2 contains nomenclature.

for an L–Pt–L bond angle of 141°; Figure 6 indicates the change in these orbital energies with angle.

Classification of molecular orbitals for L_2PtXY as bonding, nonbonding, or antibonding by inspection of the wavefunctions was not always straightforward for two reasons. First, certain wavefunctions contain significant contributions from platinum 6s and 6p atomic orbitals, and the internal nodes of these orbitals complicated their interpretation. These internal nodes are qualitatively most obvious around platinum in the $4b_2$ orbital of $(H_3P)_2PtH_2$ (Figure 2) and are due to the $6p_y$ orbital. Although there are obvious nodes between Pt and both H and P in the electron density plot for this orbital, the Pt–H and Pt–P interactions are *bonding*. In other orbitals, it was not always possible to identify the origin of the nodes by inspection. Second, for orbitals containing a significant contribution from the platinum $5d_{z^2}$ atomic orbital, it is possible to have coexisting bonding and antibonding contributions reflecting overlap of the ligand orbital with the torus or the central lobe of the platinum-centered d orbital.

The origin and character of the nodes in these orbitals was clarified by a procedure which is illustrated in Figure 7 for $(H_3P)_2PtH_2$. The eigenvalues were recalculated for new geometries in which bonds of interest were selectively stretched. For example, *increasing* the Pt–H distance of L_2PtH_2 *lowers* the energy of the $6a_1$ orbital. We conclude, then, that this orbital is antibonding with respect to the platinum–hydrogen interaction. To estimate the strength of the bonding (antibonding) interaction between two nuclei, we relied on two

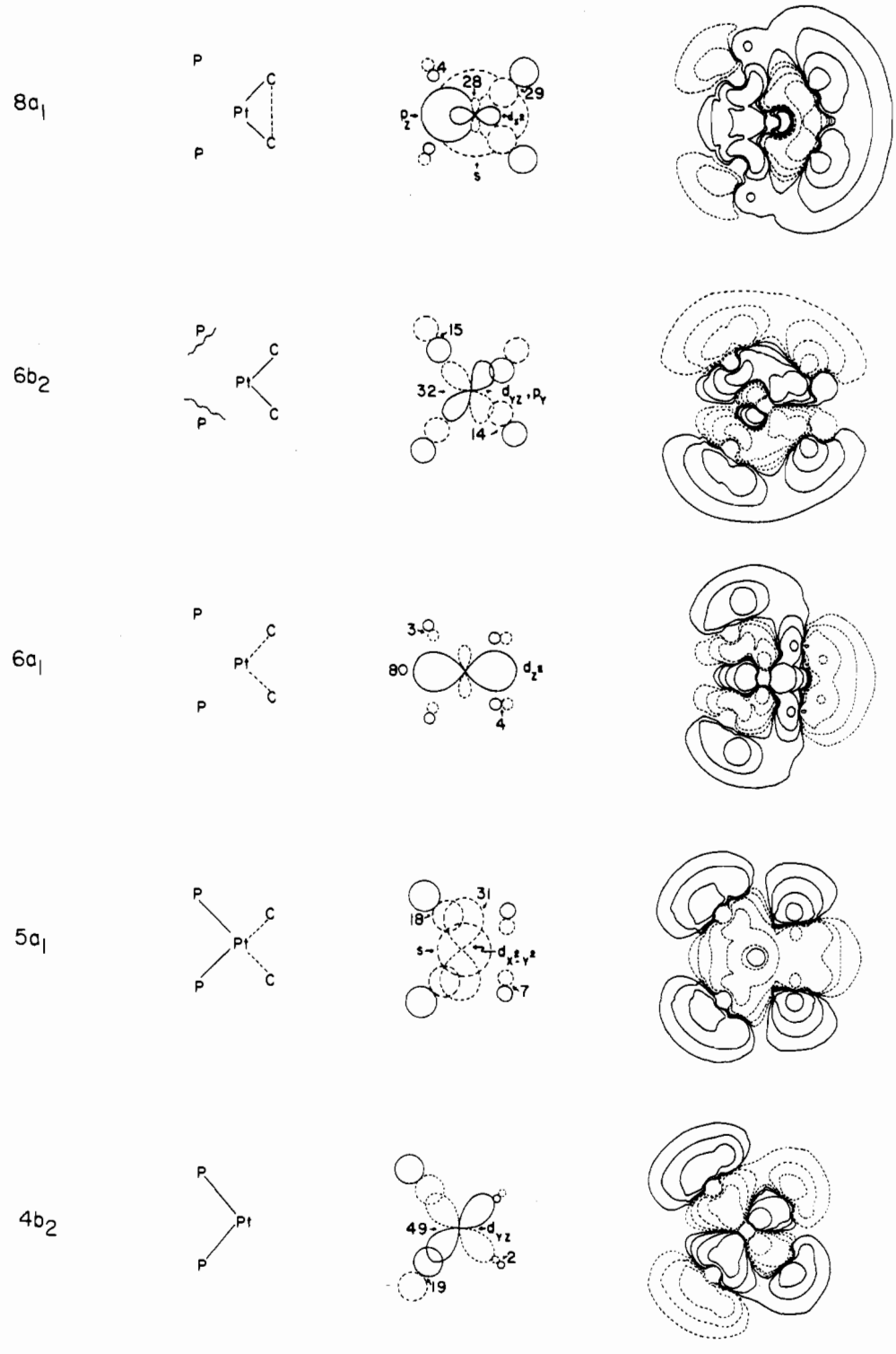

Figure 4. Orbitals important to bonding in $L_2Pt(CH_3)_2$. The caption for Figure 2 contains nomenclature.

criteria. One was the magnitude of the change in energy which accompanied a small change in bond length (Figure 7): orbitals whose energies were sensitive to these changes were considered relatively (anti)bonding. The second was the amount of charge indicated to lie between the nuclei in the contour diagrams (Figures 2–4): if these diagrams showed a significant area (volume) at the highest contour level (for example, between platinum and hydrogen in the $2b_2$ orbital of L_2PtH_2), the orbital was considered bonding.

To further ascertain if the M–X(Y) interaction in the HOMO was bonding or antibonding, we turned to the eigenvalue diagrams, Figures 1 and 9. If the L_2MXY HOMO lies higher in energy than the component L_2M and XY levels, the HOMO was identified as M–X(Y) antibonding. Such is the case for the $6a_1$ level in L_2PtH_2 (see Figure 1). If on the other hand, the L_2MXY HOMO lies significantly below the component L_2M and XY orbitals, the HOMO was identified as M–X(Y) bonding. Note that the $8a_1$ in $L_2Pt(CH_3)_2$ fits this description. If, however, the L_2MXY HOMO lies between the component energy levels [see the 12a level in $L_2PtH(CH_3)$] or at approximately the same energy as one of the component orbitals, *some* degree of M–X(Y) antibonding is indicated.

Having identified the molecular orbitals responsible for bonding platinum to hydrogen and carbon in these complexes, it is possible to interpret orbital correlation diagrams describing the conversions $L_2PtXY \rightarrow L_2Pt + XY$ (Figure 8). These

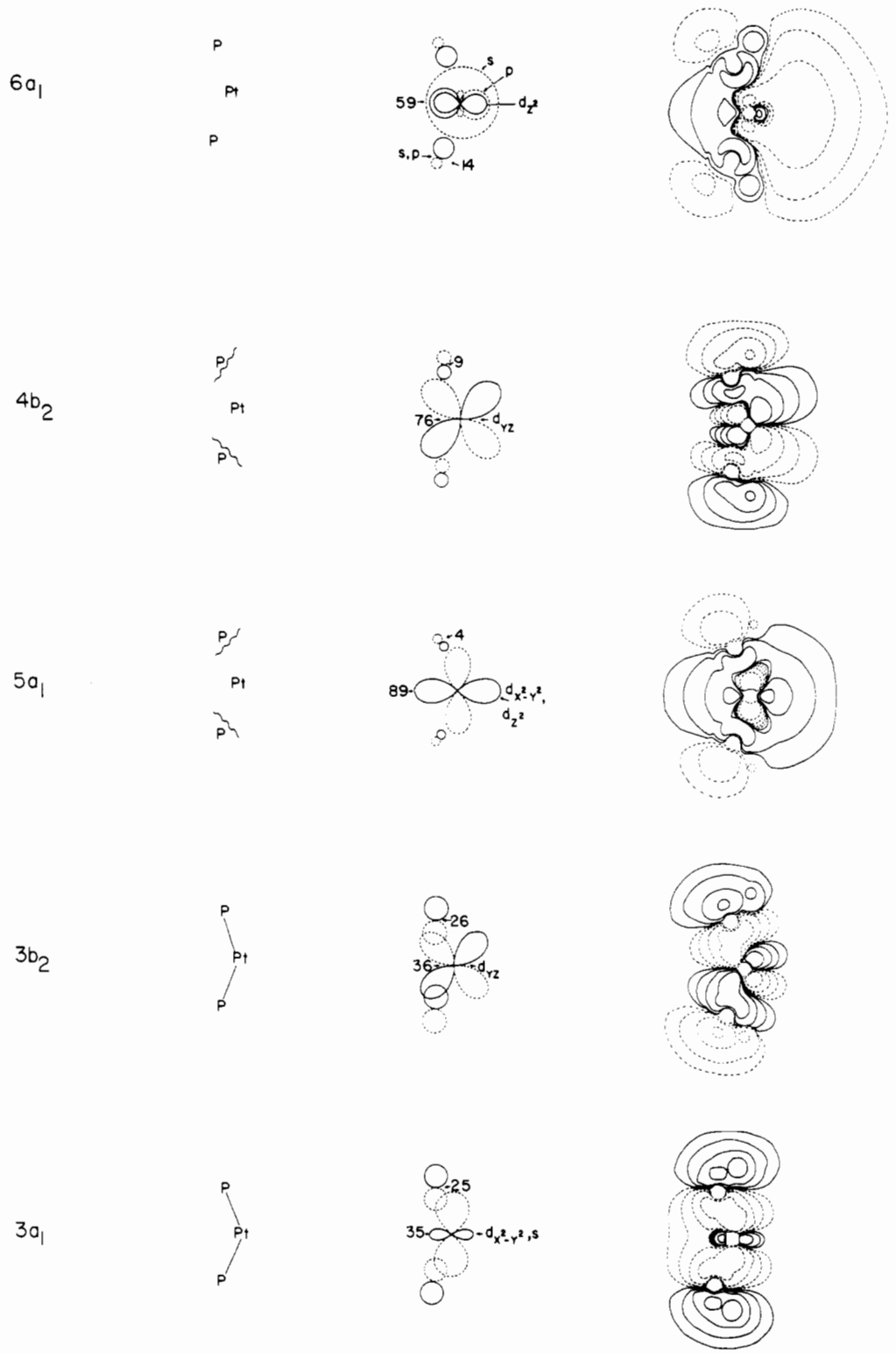

Figure 5. Orbitals for L_2Pt^0 for angle LPtL = 141°. The caption for Figure 2 contains nomenclature.

calculations contain an arbitrary element: as indicated earlier, we do not know the LPtL bond angle of the L_2Pt fragment produced as a product. Orbital correlations are given for two extremes: one having the L–Pt–L angle corresponding to the starting material ($\angle$LPtL $\simeq$ 90°) and the second to that of the final, relaxed, product ($\angle$LPtL $\simeq$ 180°). The information summarized in Figure 6 indicates that choosing another bond angle will not significantly influence the conclusions, particularly insofar as only the *relative* rates of decomposition of the three platinum complexes are of interest.

Figures 1–4 and the orbital correlation diagrams of Figure 8 contain several items of information relevant to the elimination of X–Y from L_2PtXY. First, the orbital correlation diagrams indicate that all three eliminations considered are allowed by orbital symmetry. Second, Figures 1–4 imply that the strength of the bonding between Pt and X(Y) is not due to a single orbital but represents the sum of interactions in several orbitals. Third, these figures suggest a definite difference in the distribution of Pt–X(Y) bonding, nonbonding, and antibonding contributions among these orbitals. For $L_2Pt(CH_3)_2$, the upper orbitals have Pt–CH_3 bonding character and there are no occupied Pt–CH_3 antibonding orbitals. For L_2PtH_2, the highest occupied orbital is Pt–H antibonding, and the lower ones are Pt–H bonding. For $L_2Pt(H)CH_3$, an in-

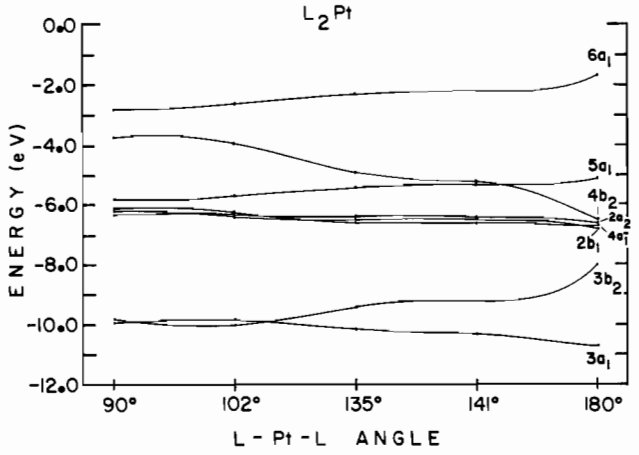

Figure 6. Eigenvalues for L_2Pt^0 as a function of angle LPtL.

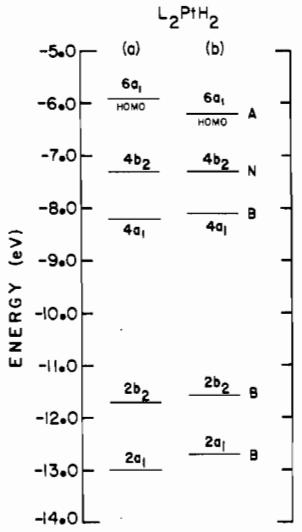

Figure 7. Response of the eigenvalues of L_2PtH_2 (a) to a 10% increase in the Z coordinate of the hydrogen atom (b). The Z axis is the direction in which the H_2 moiety leaves (see the top of Figure 1 for the coordinate axes). These shifts in energies were used to classify the energies as bonding (B), nonbonding (N), or antibonding (A) with respect to the Pt–H interactions.

termediate situation is observed. Thus, these figures contain the suggestion that the relative rates of reductive elimination (that is, essentially, the relative thermal instabilities) from these complexes correlate with the occupancy of Pt–X(Y) antibonding orbitals.

$L_2Pd(CH_3)_2$ and $L_2Ni(CH_3)_2$. Figure 9 gives eigenvalues, and Figures 10 and 11 summarize information concerning wavefunctions; Figure 12 gives orbital correlation diagrams for reductive elimination. All are given in forms analogous to those used with $L_2Pt(CH_3)_2$ to facilitate comparison.

The inferences from the calculations for $L_2Pd(CH_3)_2$ and $L_2Ni(CH_3)_2$ are similar to those for the platinum complexes. The orbital correlation diagrams indicate that all of the reactions are allowed by orbital symmetry. Examination of the occupied orbitals indicates that the HOMO of $L_2Ni(CH_3)_2$ (the $8a_1$ orbital) is weakly antibonding with respect to the C–Ni bond (the orbital is predominantly a nickel d_{z^2} orbital, with relatively little electron density on carbon). The orbitals of $L_2Pd(CH_3)_2$ and $L_2Pt(CH_3)_2$ are qualitatively indistinguishable: neither has identifiable occupied M–C antibonding orbitals.

Discussion

The bonding between M and X(Y) in L_2MXY seems to be distributed among a number of orbitals of similar energies. To the extent that the rates of reductive elimination from these

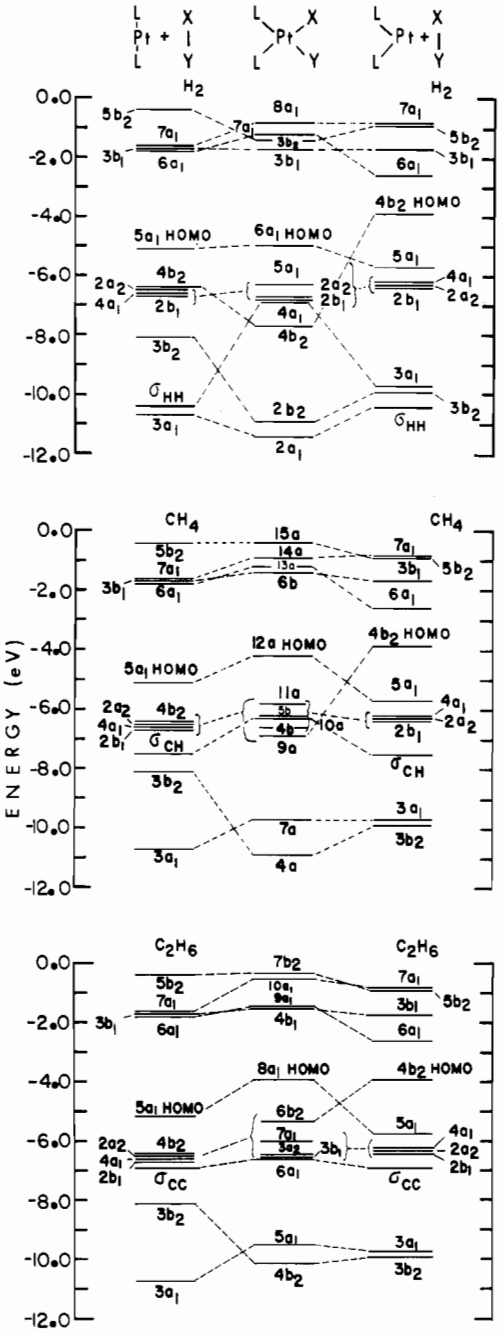

Figure 8. Orbital correlations diagrams for decompositions of L_2PtXY to XY and L_2Pt (angle = 102° and 180°). XY is in its ground-state geometry.

complexes are determined by their electronic structure, these rates are *not* expected to be entirely controlled by the properties of the HOMO or by orbital symmetry considerations but rather by the collective action of several valence orbitals. Nonetheless, a limited number of these orbitals undoubtedly are particularly important. Orbitals with the character of **1**

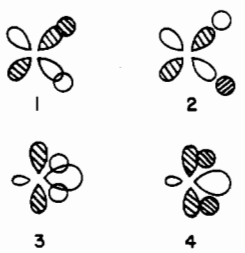

or **2** are clearly important bonding and antibonding orbitals;

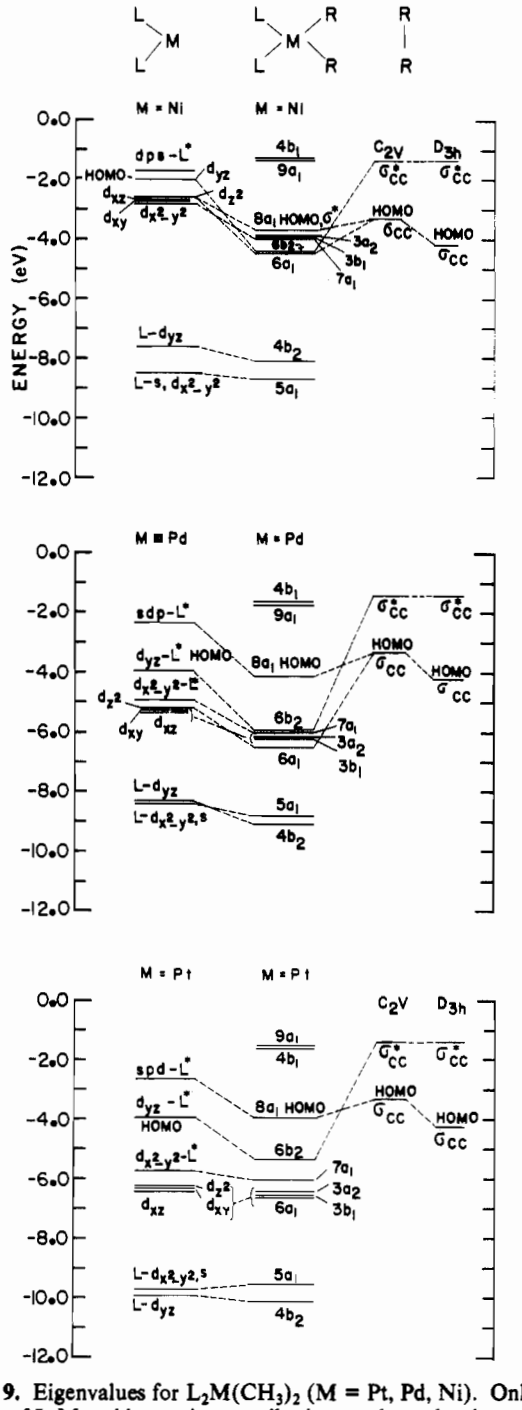

Figure 9. Eigenvalues for $L_2M(CH_3)_2$ (M = Pt, Pd, Ni). Only the orbitals of L_2M making major contributions to the molecular orbitals of $L_2M(CH_3)_2$ are indicated. L = PH_3 in each instance.

molecular orbitals formed from combinations of d_{z^2}, $d_{x^2-y^2}$, s, and p atomic orbitals on the metal (**3**, **4**) also appear from the orbital contour diagrams to be able to contribute significantly to bonding or antibonding.

One clear correlation emerges from this work relating molecular orbital structure to rates of reductive elimination. Compounds which decompose rapidly (L_2PtH_2, $L_2Ni(CH_3)_2$) have occupied orbitals with antibonding M–X character; compounds which decompose slowly ($L_2Pt(CH_3)_2$) have occupied M–X bonding orbitals and vacant M–X antibonding orbitals. In the simplest terms, this correlation is almost trivial: it implies that compounds in which the M–X(Y) bonds are weak decompose more rapidly than those in which these bonds are strong.[22] The interesting question then becomes what is the basis in atomic or molecular structure for the changes in molecular electronic structure which are reflected in the occupancy of antibonding orbitals? We *hypothesize* that the difference between the energies of the interacting orbitals of M and X(Y) is one determinant. Figure 13 summarizes the argument which forms the basis for this hypothesis in a highly simplified and schematic way. Consider a group of orbitals for the L_2Pt moiety ($\angle \simeq 90°$) of L_2PtX_2 and the σ_g HOMO (*a* symmetry) for the X_2 moiety. Assume, for simplicity, that the σ_g orbital interacts *only* with the L_2Pt of the correct symmetry closest to it in energy. (Strong interaction between orbitals of similar energies is usually rationalized on the basis of orbital size and overlap.[26] In this instance, since Pt and H or CH_3 have somewhat different orbital sizes, this assumption is not strictly justifiable. Nonetheless, the qualitative argument remains.) If it is an *occupied* orbital (of the correct symmetry for overlap) of the L_2M complex which matches the σ_{X_2} orbital most closely in energy, the resulting M–X bonding and antibonding orbitals may both be occupied (Figure 13A, exemplified by L_2PtH_2 and $L_2Ni(CH_3)_2$). If it is an *unoccupied* L_2M orbital which lies closest in energy to σ_{X_2} (Figure 13B, $L_2Pt(CH_3)_2$, $L_2Pd(CH_3)_2$) or if the HOMO of L_2M interacts strongly with $\sigma_{X_2}{}^*$ (Figure 13C; note the $6b_2$ level in $L_2Pt(CH_3)_2$), the $\sigma_{MX_2}{}^*$ orbitals resulting from these interactions should be vacant. Thus, in brief, if the orbital electronegativities are similar for σ_{X_2} and the highest occupied L_2M orbital of the same symmetry, the MX_2 fragment can be expected to have an occupied antibonding orbital and to be unstable with respect to reductive elimination; if these orbital electronegativities are enough different that one of the strongly interacting pair of high-lying orbitals is vacant, the MX_2 fragment should have a vacant antibonding orbital and be relatively stable to reductive elimination. In other terms, the interaction suggested by Figure 13A is predominantly covalent while that in Figure 13B, C has more or less ionic character.

Reference to Figures 2, 4, 10, and 11 indicate that the important elements in these energy level diagrams are approximated by the interactions outlined in Figure 13, although they are obviously more complicated, since several L_2M orbitals have the correct symmetry to interact with σ_{X_2} and $\sigma_{X_2}{}^*$.

Inspection of calculated charges in the several complexes examined here supports these hypotheses concerning the importance of electronegativities (Table I). For the series $L_2M(CH_3)_2$, the complex in which the *least* charge transfer from carbon to metal would take place during reductive elimination is $L_2Ni(CH_3)_2$; this complex is also the one for

Table I. Calculated Atomic Charges in Complexes of the Structure L_2PtXY (L = PH_3, X, Y = H, CH_3)

complex	P	M	C	H
L_2PtH_2	0.28+	0.20–		0.04–
L_2PtHCH_3	0.298+	0.160–	0.107–	0.024–
$L_2Pt(CH_3)_2$	0.28+	0.001–	0.176–	
$L_2Pd(CH_3)_2$	0.27+	0.061–	0.140–	
$L_2Ni(CH_3)_2$	0.44+	0.59–	0.013–	
H_2				0.0
$(H_C)_3CH$			0.174+	0.129–[a]
C_2H_6[b]			0.177+	0.067–
L_2Pt (90°)	0.393+	0.439–		
L_2Pt (102°)	0.403+	0.460–		
L_2Pt (180°)	0.422+	0.521–		
L_2Pd (102°)	0.525+	0.559–		
L_2Ni (102°)	0.372+	0.601–		

[a] The value for H_C is 0.013+. The C–H distance assumed is 2.73 Å and corresponds to the stretched value in $L_2Pt(H)CH_3$. [b] The assumed C–C distance is 2.72 Å and corresponds to the value in $L_2Pt(CH_3)_2$.

(26) Hoffmann, R. *Acc. Chem. Res.* **1971**, *4*, 1–9. Hetlbronner, E.; Bock, H. "The HMO Model and Its Application"; Wiley-Interscience: New York, 1976.

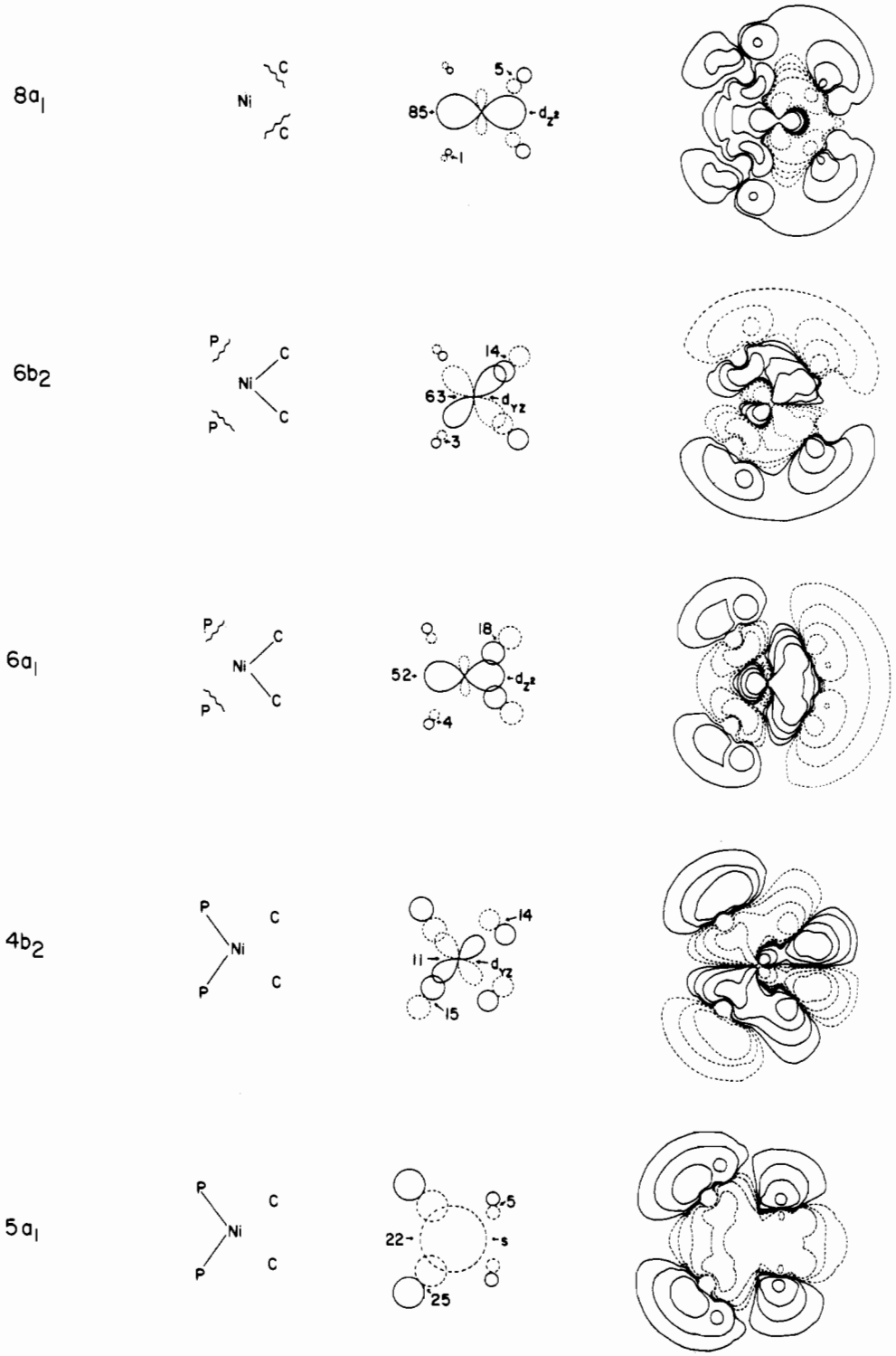

Figure 10. Orbitals important to bonding in $L_2Ni(CH_3)_2$. The caption for Figure 2 contains nomenclature.

which reductive elimination is most rapid. For the series L_2PtXY, the complex for which the least charge is transferred to the metal during reductive elimination is L_2PtH_2. This complex is also the one which reductively eliminates most rapidly of the series containing platinum.

This model correlates the rates of reductive elimination with the presence of occupied M–X(Y) antibonding orbitals and by inference with the relative electronegativities of the L_2M orbitals and the "stretched" σ_{XY} orbital. It hypothesizes that the relative electronic energies of the starting materials determine the rates of these reductive elimination reactions. A number of other possible models for these reactions might, of course, also be considered. Several of these follow. We note that each of the factors emphasized in these models undoubtedly contributes to some extent to the rates of these reactions and that they are not necessarily orthogonal.

(1) Exothermicity. The reaction rate for the decomposition of L_2MXY might correlate with the free energies of these reactions: such correlations are numerous in kinetics, although they usually apply only to a restricted range of variations in the reactant.[27] The arguments presented in this paper deal

(27) Hine, J. "Structural Effects on Equilibria in Organic Chemistry"; Wiley-Interscience: New York, 1975. Lowry, T. H.; Richardson, K. S. "Mechanism and Theory in Organic Chemistry"; Harper and Row: New York, 1976. Norton (ref 5) has discussed possible correlations between rates and exothermicities of organic reactions.

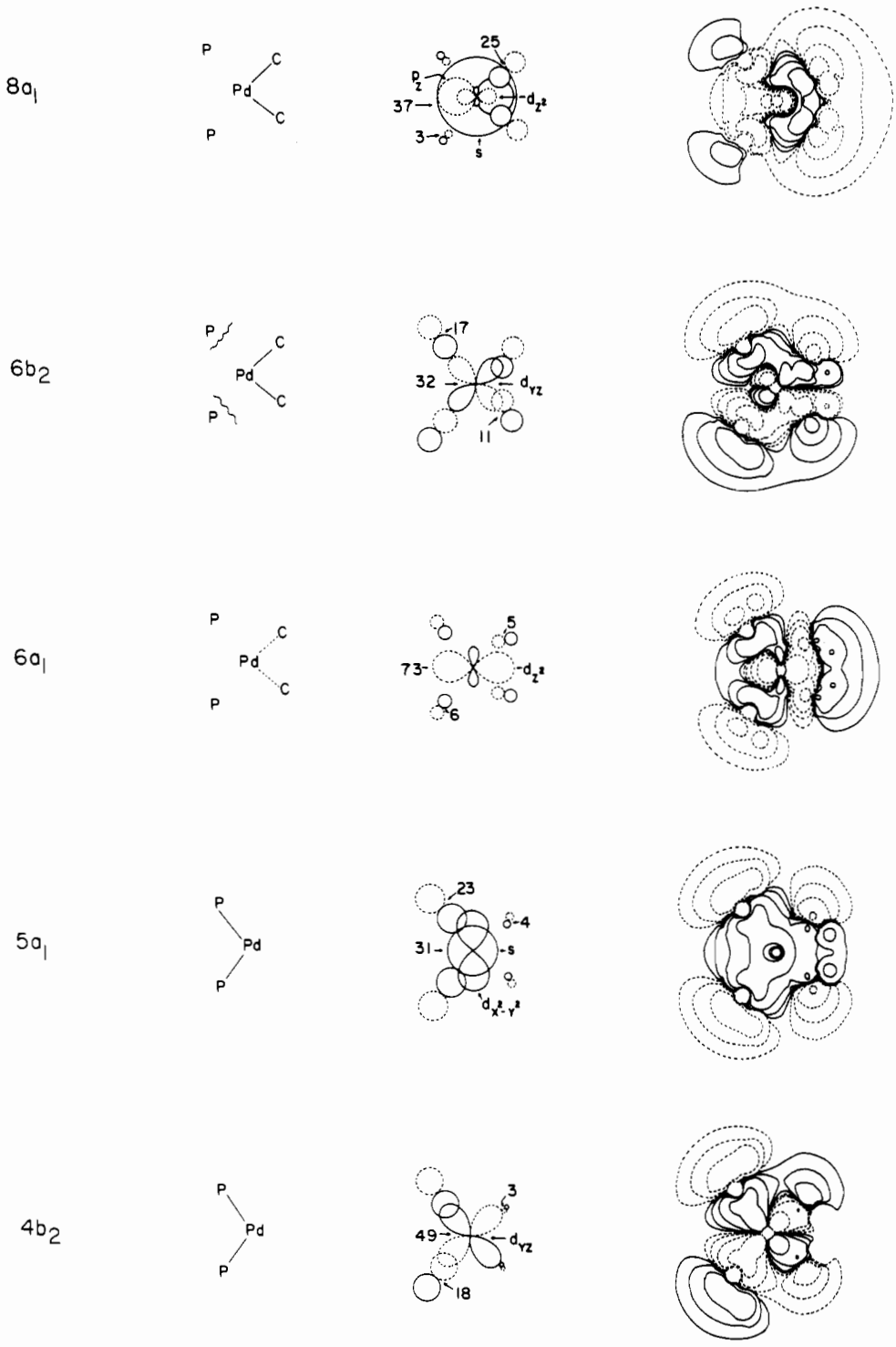

Figure 11. Orbitals important to bonding in $L_2Pd(CH_3)_2$. The caption for Figure 2 contains nomenclature.

with only one contribution to this free energy: viz, the enthalpy of the reactants. The enthalpies of the products are the second contributor; we note that the bond energies of the products (kcal mol^{-1}: $D_{H-H} = 104 = D_{H_3C-H} = 104 > D_{H_3C-CH_3} = 88$) do not seem to correlate well with the rates of decomposition of L_2PtXY, but we caution that the series is too small to provide the basis for convincing generalizations. The relative rates of decomposition might, in principle, be dominated by the relative energies of either the starting materials or the products. The data needed to identify the more important contributor are not available in the series examined here. Nonetheless, comparison of our results with those obtained by Hoffmann et al.[9] using extended Hückel methods suggest that in at least some areas the response of the transition state to changes in structure may be more like that of products than reactants (see below).

(2) Relief of Steric Strain. Changes in nonbonded interactions within crowded transition-metal complexes are known to be of major importance in determining the rate of many organometallic reactions, including reductive eliminations and oxidative additions.[2,8] The differences in size of H and CH_3 and of Pt(II), Pd(II), and Ni(II) could in principle result in contributions to rates from nonbonded interactions between X(Y) and L larger than those due to differences in bond energies.

(3) Electronic Effects of Particular Importance in the Transition State. Of the many such effects which could be imagined a priori, one in particular is suggested by the contour

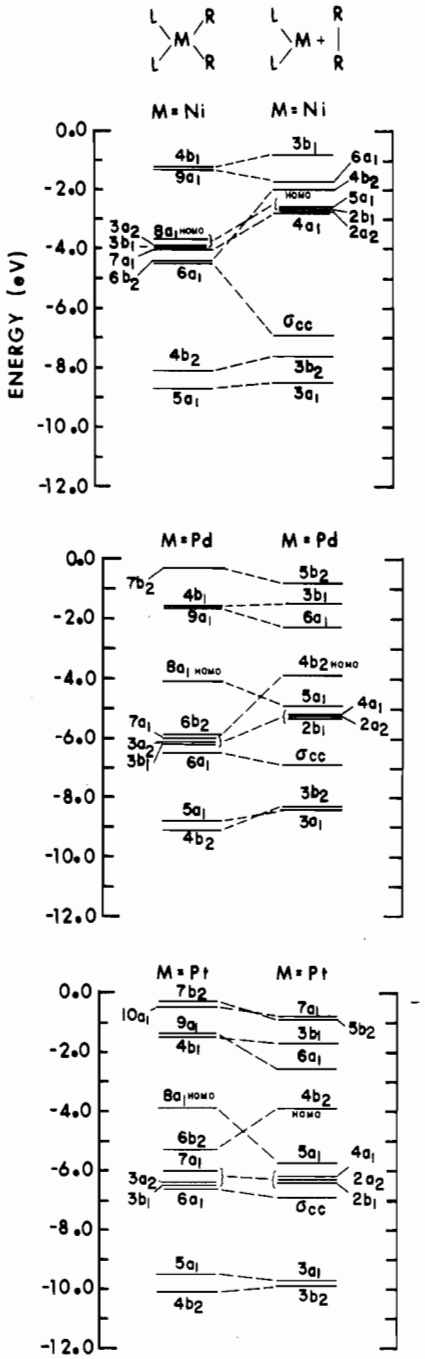

Figure 12. Orbital correlation diagrams for decomposition of $L_2M(CH_3)_2$ to C_2H_6 and L_2M (angle = 102°). C_2H_6 is in its ground-state geometry.

diagrams of Figures 2–4. During reductive elimination, the X–Y group forms a bond. The 1s orbital on hydrogen is spherically symmetrical; the p (or sp^3) orbitals on carbon are not. Thus, three-center bonding of the type **5** might be more

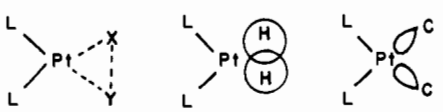

5 **6** **7**

important for hydrogen (**6**) than methyl (**7**). The $6a_1$ of L_2PtH_2 shows some evidence of H–H bonding in the ground state; a corresponding concentration of charge between the carbon atoms of $L_2Pt(CH_3)_2$, or between the carbon and hydrogen of $L_2Pt(H)CH_3$, is not evident. That the L_2PtH_2 complex may in fact have a C_{2v} transition state with symmetric

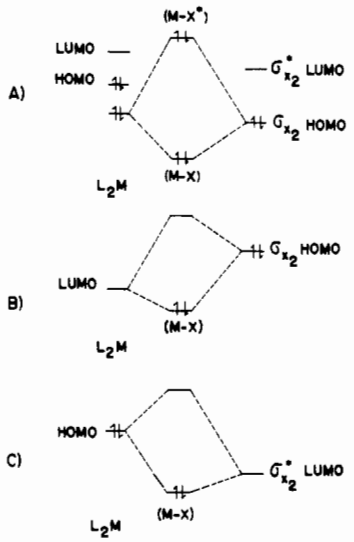

Figure 13. Schematic energy level diagram summarizing the important interactions in L_2MXY.

Pt–H bonds is supported by recent ab initio calculations performed by Noell and Hay[12] on the reverse reaction $H_2 + Pt(PH_3)_2 \rightarrow cis\text{-}Pt(PH_3)_2H_2$. Here, the symmetric C_{2v} configuration was found to provide the lowest energy transition state.

Brief comparison of our results with those of Hoffmann et al.[9] is useful. Hoffmann reached three major conclusions: (1) the more strongly electron donating is X (and Y), the more rapid is reductive elimination; (2) the more strongly electron donating is L, the slower is reductive elimination; (3) the barrier to reductive elimination is determined in major part by b_2 orbitals of type **1**. The first two of these conclusions have some experimental support. In general, the complexes L_2MX_2 are more stable for X = CF_3,[28] Cl, and Ph than for X = CH_3; Halpern et al. have reported that the rate of loss of methane from $(XPh_3P)_2Pt(CH_3)H$ is more rapid when X is electron withdrawing. Our calculations apply only to the electronic structures of the reactants. A *large* (several electronvolts) lowering in the energy of the X(Y) orbitals or a large increase in the energy of the L_2M orbitals should increase the probability that PtXY antibonding orbitals are occupied and predict a destabilization of the complexes. The influence of *small* changes of the type encountered in substituents is not obvious. Qualitatively, since charge density on the metal center of L_2M is larger than that in L_2MXY, electron-donating L should destabilize the product more than the reactant. Similarly, since reductive elimination involves charge transfer from X(Y) to metal, the more electron-withdrawing X(Y) is, the more stable should L_2MXY be. Thus, the results of our studies provide an adequate ad hoc rationalization of observed substituent effects and can be interpreted to be consistent with the potential surfaces calculated by Hoffmann et al. They do not, however, lend themselves easily to predictions of rate differences resulting from small perturbations in substituent structure. The third conclusion of Hoffmann, that the energy of an orbital of type **1** dominates the changes in energy in going from reactant to transition state, cannot be compared with our results since we do not calculate total energies.

Acknowledgment. This work was supported by NSF (Grant DMR-78-24185). We thank Dr. Dimitri Vvedensky for many valuable discussions.

Registry No. L_2PtH_2, 76832-29-6; L_2PtHCH_3, 79232-17-0; $L_2Pt(CH_3)_2$, 79232-18-1; $L_2Pd(CH_3)_2$, 79218-06-7; $L_2Ni(CH_3)_2$, 79218-07-8.

(28) Cullen, W. R. *Adv. Inorg. Chem. Radiochem.* **1972**, *15*, 323–374.

Supplementary Material Available: Reviewers' comments and authors' reply during evaluation of this work, comprising an instructive dialogue on the relative merits of the present approach as compared to other theoretical studies of this type. At the suggestion of Reviewer No. 2 and with concurrence of all parties involved, these materials are offered as a supplement (19 pages) to this article; ordering information is given on any current masthead page. In considering this suggestion the Reviewers were asked and have agreed to reveal their identities: Reviewer No. 2, R. Hoffmann; Reviewer No. 1, W. A. Goodard, III.

Contribution from the Departments of Chemistry, The College of Wooster, Wooster, Ohio 44691, and The University of Toledo, Toledo, Ohio 43606

Ligand-Bridged Dimers of Pentacarbonyltungsten. Synthesis and Characterization[1]

P. L. GAUS,*[2a] J. M. BONCELLA,[2a] K. S. ROSENGREN,[2a] and M. O. FUNK[2b]

Received August 4, 1981

Monomeric and dimeric derivatives of the type $W(CO)_5L$ and $[W(CO)_5]_2L$ have been synthesized by a method involving the photochemical generation of the intermediate solvent adduct $W(CO)_5THF$. In each case L is a bifunctional nitrogen heterocycle such as 4,4′-bipyridine. The monomers and dimers were characterized by HPLC, ^1H NMR, ^{13}C NMR, elemental analysis, and electronic spectroscopy. One of the most interesting features of the electronic spectra of the dimers is that the metal-to-ligand charge-transfer absorption occurs at a significantly lower energy than the ligand field band at 405 nm for the dimers $[W(CO)_5]_2L$ containing the conjugated bridging ligands 4,4′-bipyridine and 1,2-bis(4-pyridyl)ethylene.

Introduction

The photosubstitutional reactivity of the zerovalent metal carbonyl complexes $M(CO)_5L$ is not only dependent on the wavelength but also dependent on the nature of the unique ligand L. Both Wrighton[3] and Zink[4] have examined the photosubstitution reactions of these compounds where M = W and L = a nitrogen heterocycle. Wrighton[3] first identified the metal-to-ligand charge-transfer (MLCT) state as being photochemically unreactive. Zink[4] later noted a correlation between (1) the relative positions of the metal-to-ligand charge-transfer absorption bands and the ligand field (LF) absorption bands in the tungsten compounds and (2) the quantum yields for both unique ligand and carbonyl ligand photosubstitution.

Accordingly, Zink[4b] has proposed a classification (based on the nature of the unique ligand L) of the photochemistries of the compounds $W(CO)_5L$. Compounds that fall into Zink's class 3(2) have metal-to-ligand charge-transfer absorption bands at lower energy than ligand field ($^1E \leftarrow {}^1A$) bands. Instead of efficient unique-ligand (L) substitution as is observed for Zink's class 1 compounds (such as the case where L = piperidine), class 3(2) compounds undergo both unique-ligand and CO photosubstitution reactions with extremely low ($\phi < 0.02$) quantum yields, when the irradiation wavelength corresponds to the lowest energy feature of the absorption spectra. There are, however, few examples of compounds that fall into Zink's class 3(2).

We report here on the synthesis and characterization of some new "class 3" homonuclear dimers of the general formula $[W(CO)_5]_2L$, where L = 4,4′-bipyridine (BPY), 1,2-bis(4-pyridyl)ethane (BPA), or 1,2-bis(4-pyridyl)ethylene (BPE).

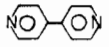

BPY

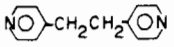

BPA

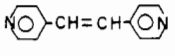

BPE

The dimers and the monomeric compound $W(CO)_5BPY$ have been characterized by elemental analysis, HPLC, electronic spectra, ^1H NMR, and ^{13}C NMR. In specific cases, the metal-to-ligand charge-transfer band of a dimer is lower in energy than the ligand field absorption bands. Our intent is to extend the number of compounds that fall into Zink's class 3 and then, in a related paper, to examine the photochemical reactivities of such compounds. Recently, similar dimers have been reported,[5] as well as monomeric derivatives[6] for which the MLCT band appears at significantly lower energy than LF bands in the electronic spectrum.

Experimental Section

Materials and Reagents. The starting hexacarbonyl, $W(CO)_6$, was obtained from Strem Chemicals and was used without further purification. The free ligands BPA and BPE were obtained from Aldrich and used without purification. The ligand BPY (Aldrich) was dissolved in THF, and the resulting solution was dried over 4-Å molecular sieves and under an atmosphere of dry nitrogen gas because the ligand was available only as the dihydrate. All THF solvent was distilled from $LiAlH_4$ and stored under dry nitrogen gas. THF was transferred under an atmosphere of dry nitrogen gas with syringe techniques. All solvents used in the syntheses were ACS reagent grade or better and were used without further purification. Solvents for HPLC and those for spectra were spectrophotometric grade.

Photolyses were carried out with a 450-W Hanovia medium-pressure mercury vapor lamp that was housed in an Ace Glass quartz immersion well. The photolyses were performed under an atmosphere of dry nitrogen gas. All of the products of the photolyses were handled in the dark or with a minimum amount of dim red light.

Synthetic Procedures. (a) $[W(CO)_5]_2L$. The homonuclear dimers were prepared by the general synthetic procedure in which a dry THF solution of the free ligands BPY, BPA, or BPE was thermally reacted with a THF solution of the solvent adduct, $W(CO)_5THF$.[7] The intermediate product $W(CO)_5THF$ was not isolated. A specific

(1) Presented in part at the Second Chemical Congress of the North American Continent, Las Vegas, NV, Aug 1980; see Abstracts, INOR 334.
(2) (a) The College of Wooster. (b) The University of Toledo.
(3) Wrighton, M. S.; Abrahamson, H. B.; Morse, D. L. *J. Am. Chem. Soc.* **1976**, *98*, 4105–4109.
(4) (a) Dahlgren, R. M.; Zink, J. I. *Inorg. Chem.* **1977**, *16*, 3154–3161. (b) Dahlgren, R. M.; Zink, J. I. *J. Am. Chem. Soc.* **1979**, *101*, 1448–1454.
(5) (a) Keiter, R. L.; Kaiser, S. L.; Hansen, N. P.; Brodack, J. W.; Cary, L. W. *Inorg. Chem.* **1981**, *20*, 283–284. (b) Bataglia, R.; Kisch, H.; Krueger, C.; Liu, K. K. *Z. Naturforsch., B.: Anorg. Chem., Org. Chem.* **1980**, *35*, 719–723. (c) Daamen, H.; Stufkens, D. J.; Oskam, A. *Inorg. Chim. Acta* **1980**, *39*, 75–80. (d) Sellmann, D.; Gerlach, R.; Jodden, K. *J. Organomet. Chem.* **1979**, *178*, 433–447. (e) Pannell, K. H.; Iglesias, R. *Inorg. Chim. Acta* **1979**, *33*, L161–L162. (f) Ernhoffer, R.; Shepherd, R. E. *J. Chem. Soc., Chem. Commun.* **1978**, 859–861. (g) Ackermann, M. N.; Kou, L. *Inorg. Chem.* **1976**, *15*, 1423–1427. (h) Ehrl, W.; Rinck, R.; Vahrenkamp, H. *J. Organomet. Chem.* **1973**, *56*, 285–293. (i) Fowles, G. W. A.; Jenkins, D. K. *Inorg. Chem.* **1964**, *3*, 257–259. (j) Chatt, J.; Watson, H. R. *J. Chem. Soc.* **1961**; 4980–4988.
(6) (a) Maetens, D.; Nasielski, J.; Nasielski-Hinkens, R. *J. Organomet. Chem.* **1979**, *168*, 177–181. (b) Pannell, K. H.; Gonzalez, M.; Leano, H.; Iglesias, R. *Inorg. Chem.* **1978**, *17*, 1093–1095.
(7) Strohmeier, W. *Angew. Chem.* **1964**, *76*, 873–881.

0020-1669/82/1321-2174$01.25/0